

REPORT DOCUMENTATION PAGE

AFRL-SR-BL-TR-99-

0306

Public Reporting burden for this collection of information is estimated to average 1 hour per response, including the time for reviewing existing information, searching existing data sources, gathering and maintaining the data needed, and completing and reviewing the collection of information. Send comment regarding this burden estimate or any other aspect of this collection of information, including suggestions for reducing this burden, to Washington Headquarters Services, Directorate for Information Operations and Reports, 1215 Jefferson Davis Highway, Suite 1204, Arlington, VA 22202-4302, and to the Office of Management and Budget, Paperwork Reduction Project (0704-0188), Washington, DC 20503.

1. AGENCY USE ONLY (Leave Blank)		2. REPORT DATE 12/16/99		3. REPORT TYPE AND DATES COVERED Final Technical Report; 1 Apr 96-30 Sep 99	
4. TITLE AND SUBTITLE Interface formation and solid-solid reactions induced by cluster ion deposition				5. FUNDING NUMBERS F49620-96-1-0119	
6. AUTHOR(S) Scott L. Anderson				8. PERFORMING ORGANIZATION REPORT NUMBER None	
7. PERFORMING ORGANIZATION NAME(S) AND ADDRESS(ES) University of Utah, Chemistry Department 315 S. 1400 E. RM Dock, Salt Lake City, UT 84112				10. SPONSORING / MONITORING AGENCY REPORT NUMBER	
9. SPONSORING / MONITORING AGENCY NAME(S) AND ADDRESS(ES) AFOSR/NL 801 North Randolph Street, Room 732 Arlington VA 22203-1977				10. SPONSORING / MONITORING AGENCY REPORT NUMBER	
11. SUPPLEMENTARY NOTES					
12 a. DISTRIBUTION / AVAILABILITY STATEMENT Approved for public release; distribution unlimited.				12 b. DISTRIBUTION CODE	
13. ABSTRACT (Maximum 200 words) Development is reported of a unique phase-space-compressing ion deposition beamline, coupled to an ultrahigh vacuum surface preparation/analysis system. The performance of the beamline in low energy focused deposition is discussed. A system of transferrable, high precision sample holders is described. An embedded-atom code developed for simulation of the cluster impact behavior is described. Initial results are presented for deposition, sticking, and penetration of copper atoms and copper dimers impacting on molybdenum and nickel over a wide range of collision energies.					
14. SUBJECT TERMS ion beams, deposition, film growth, implantation, sputtering, clusters				15. NUMBER OF PAGES 12	
				16. PRICE CODE	
17. SECURITY CLASSIFICATION OF REPORT UNCLASSIFIED	18. SECURITY CLASSIFICATION ON THIS PAGE UNCLASSIFIED	19. SECURITY CLASSIFICATION OF ABSTRACT UNCLASSIFIED	20. LIMITATION OF ABSTRACT UL		

NSN 7540-01-280-5500

Standard Form 298 (Rev. 2-89)
Prescribed by ANSI Std. Z39-18
298-102

DTIC QUALITY INSPECTED 2

19991230 024

Final Report

Title: Interface formation and solid-solid reactions induced by cluster ion deposition
PI: Scott L. Anderson
Grant: F49620-96-1-0119
Organization: Chemistry Department, University of Utah
315 S. 1400 E. Rm Dock
Salt Lake City, UT 84112-0850
Phone: (801) 585-7289
Fax: (801) 581-8433
email: anderson@chemistry.utah.edu

Objective of project:

This project was designed with the goal of probing metal-metal, metal-metal nitride, and metal-metal oxide interface chemistry, relevant to growth of thin films and coatings by physical deposition processes, where mixing and bonding at the interface is driven by bombardment by high energy ions, including small clusters. In addition, the information obtained regarding penetration, mixing, and diffusion behavior should be useful in developing models of ultra low energy (<1000 eV) ion implantation – an increasingly important technology for semiconductor production. The instrument constructed is versatile, and would also make a powerful tool for studies of catalysis chemistry

Approach:

A beam of mass selected ions, either atomic or small clusters, is prepared in a novel beamline, then deposited on clean surfaces in ultra-high vacuum. For the metal-metal systems that have been the focus of our work to date, the primary analysis tool is angle-resolved electron spectroscopy. By measuring ratios of various photoelectron and x-ray-induced auger electron lines, we get several measures of the sticking probability and depth distribution. A metropolis simulated annealing algorithm is used to extract information from the data, by fitting with a full physics-based model of the electron production and propagation in the composite surface layer.

To complement the experimental work, we have also developed a classical trajectory program to simulate deposition dynamics. The target is represented by a ~400 atom slab of the metal of interest. Accurate embedded atom potentials are used to describe the interactions, and enough trajectories are run at each impact energy to give reasonable statistics for the various distributions and correlation functions. The trajectories, of course, can only probe the short time dynamics (picosecond time scale) and therefore give information only regarding the initial impact dynamics. As the experimental time scale is much longer, thermally-activated diffusion or desorption processes may significantly modify the initial depth profiles.

Results and Progress:

To date our major activities have been:

1. Design, construction, and debugging of the instrument
2. Construction and optimization of magnetron sputter/aggregation and 100 Hz laser vaporization cluster ion sources
3. Development of the embedded-atom trajectory simulation program and potentials
4. Study of Cu^+ and Cu_2^+ interactions with Mo from $E_{\text{impact}} = 7$ to 220 eV
5. Study of Cu^+ and Cu_2^+ interactions with Ni from $E_{\text{impact}} = 2$ to 220 eV
6. Development of a simulated-annealing fitting program to analyze deposition data

These activities will be discussed briefly below.

1. Instrument development:

A schematic of the instrument is shown in Fig. 1.

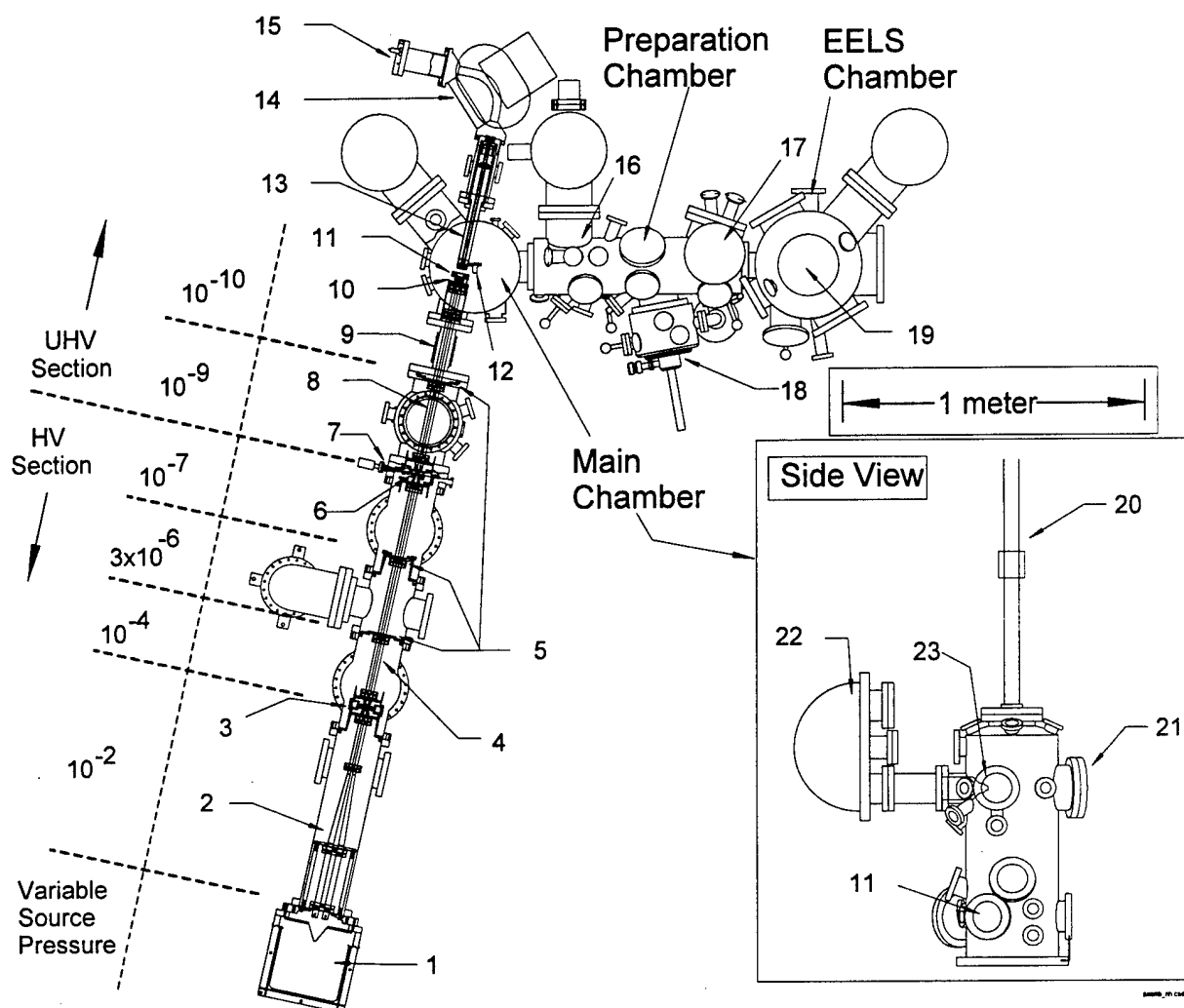


Figure 1 Utah Ion Deposition Instrument: 1. Ion source chamber, 2. Compressing quadrupole trap, 3. Einzel lens/differential pumping aperture, 4. Low pass quadrupole, 5. Mid-quad differential pumping apertures, 6. Lens/differential pumping aperture, 7. UHV-HV isolation valve (built into lens), 8. High pass quadrupole, 9. Isolation bellows, 10. Deceleration lenses and exposure mask, 11. Deposition station kinematic mount, 12. Vertical transporter sample mount, 13. Octapole ion guide, 14. Magnetic sector mass analyzer, 15. Channeltron detector, 16. Sample sputter/anneal station, 17. TPD station, 18. Load lock, 19. EELS chamber and station (manipulator not shown), 20. Vertical transporter, 21. STM station, 22. 150 mm hemispherical energy analyzer, 23. XPS/UPS/Auger station (manipulator not shown)

Beamline

Our phase-space compression method has been described elsewhere¹, the key feature being storage in a tapered rf quadrupole trap to collisionally damp both spatial and energy distributions, resulting in a large decrease in beam phase space (or normalized emittance), and corresponding increase in low energy focusability. In previous cluster ion deposition experiments, the deposition spot has been

¹K. J. Boyd, A. Lapicki, M. Aizawa, and S. L. Anderson, *Rev. Sci. Instrum* **69**, 4106 (1998).

5 - 10 mm, and the minimum energy has typically been $> \sim 10$ eV. In many of those experiments, soft-landing on a rare-gas buffer layer has been used to reduce fragmentation upon impact. For our purposes, we need to vary impact energy, thus soft landing is not an option. Our beamline allows sub-millimeter deposition spots at energies down to < 2 eV, thus increasing deliverable intensity by about two orders of magnitude, and allowing direct deposition over the full energy range of interest.

A few people have questioned whether our tapered quadrupole really does something more than a linear gas-filled quad would do. To lay this question to rest, we recently replaced the tapered quad with a conventional linear quad. The result was a substantial (factor of ~ 3) reduction in beam current density on the target. More importantly, the kinetic energy spread of the beam increased from < 1 eV to ~ 10 eV (for Cu^+ generated by sputtering), demonstrating that the tapered shape substantially enhances both collection/focusing efficiency, and cooling efficiency (due to longer trap residence times).

After compression, the beam is mass-selected by a pair of quadrupole ion guides. The first is operated as a low pass filter, rejecting clusters heavier than desired, and the second is operated as a high-pass filter. The combination is, thus, a variable bandpass mass filter. These guides also transport the beam at low energies through five differential pumping apertures into the UHV deposition chamber, using rf confining fields to prevent space charge-driven beam expansion.

Finally, the beam is focused by a set of DC ion lenses through an $800\mu\text{m}$ collimating aperture, positioned a few hundred microns in front of the sample. The deposition energy is set by biasing the target relative to the centerline potential of the compressing quadrupole guide, and is measured by retarding potential analysis. Target current is directly measured with an electrometer, and the deposition spot is profiled by small-area x-ray photoelectron spectroscopy (XPS). Deposition spots are found to have diameters closely matching the $800\mu\text{m}$ aperture size. By removing the sample from the deposition station, the cluster beam can be passed into an octapole ion guide, then into a magnetic sector spectrometer for high resolution mass analysis. Cu_2^+ beams have been deposited successfully at energies as low as 1 eV.

Surface preparation/analysis capabilities

The UHV section consists of five interconnected and isolable UHV chambers, together with a load lock. This design was made possible by the donation by Kodak of an ESCALAB II spectrometer that provided two UHV chambers, most of the pumping system, and a valuable collection of manipulators, transporters, and other UHV hardware. The system was upgraded by addition of PHI XPS hardware, an STM, a new main chamber, the beam monitor mass spectrometer, a TPD/TPR station, a new sample prep station, and the beamline.

To make use of the tightly collimated deposition beam, our analysis techniques must locate and analyze sub-millimeter sample spots. The conventional approach would be to mount the sample on a precision manipulator, however, for STM measurements, this approach is not possible. We were forced to develop a system of precision sample stations that accept kinematic interchangeable sample holders. Preparation, deposition, and analysis stages are each equipped with a sample station, and the sample is transported between them by a system of

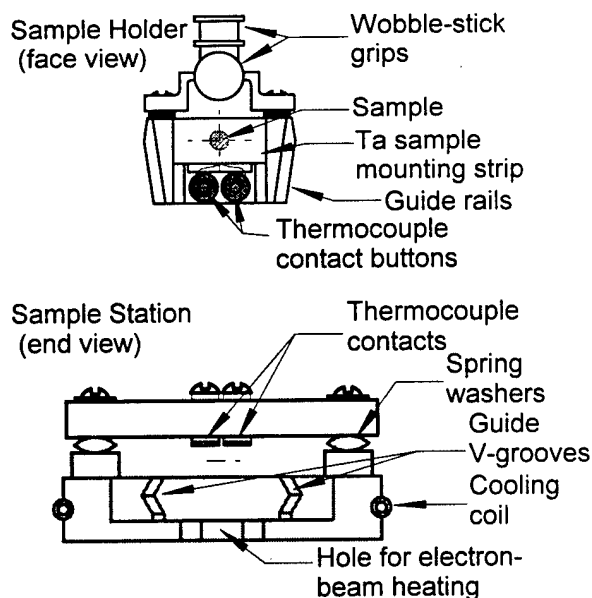


Figure 2. Sample holder and mating station

transporters and wobble stick manipulators. Positioning reproducibility is better than 50μ . An example station and holder are shown, approximately to size, in Fig. 2. A further benefit of the movable holder design, is that we can have numerous samples in the system at any given time; indeed, it is possible to have several processing steps going simultaneously on different samples.

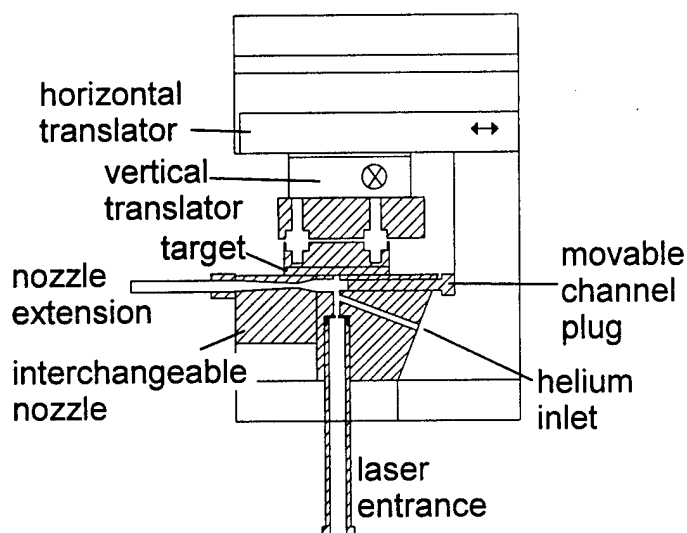
The following analysis techniques are available: scanning tunneling microscopy (STM); angle-resolved x-ray photoelectron spectroscopy (XPS) and ion-neutralization spectroscopy (INS); temperature-programmed desorption/reaction (TPD/TPR); and high resolution electron energy loss spectroscopy (HREELS). With the exception of HREELS, all these techniques are capable of small area analysis, so that we probe only the cluster-containing area of the sample. For HREELS, surface charging makes it difficult to reproducibly control the e-beam spot size and position, and difference measurements are required to identify features originating in the cluster spot. The system is also equipped with a sputter/anneal station for sample preparation, and a load-lock for sample exchange. To help reduce the gas load on the Main and EELS analysis chambers, all processes that involve high gas loads are carried out in the Prep chamber, isolated from the two analysis chambers.

2. Development of cluster ion sources.

For cost reasons, the source we developed first was a magnetron sputtering/gas aggregation source. Magnetron sputtering produces copious metal vapor and substantial fluxes of small cluster ions. The idea of the source was to aggregate the metal vapor around the small cluster ions, growing larger clusters. The problem is that under conditions where the magnetron will operate, it is impossible to control aggregation, and cluster growth proceeds such that the size distribution is dominated by clusters with 1000 to 5000 atoms. While these clusters may be of interest later, we wish to focus our initial experiments on smaller sizes. In addition, the magnetron source has very large sample consumption rate (several grams/hours) and we can only afford to operate it with metals such as copper and aluminum where we can do our own target fabrication (commercial targets lasting 8 hours cost \$300 - \$1000). Our initial deposition experiments have, therefore, been limited to studies of small copper and aluminum clusters.

DURIP funding from AFOSR has enabled us to purchase a 100Hz Nd:YAG laser (Spectra Physics LAB 190-100) suitable for pumping a laser vaporization cluster ion source. We have constructed several different geometry sources to experiment with how source behavior changes at high repetition rates. The current source is shown in Fig. 3. The source was designed to use planar targets of arbitrary shape. The target is scanned across the laser channel by a pair of stepping motors, allowing the scanning pattern to be adapted to the shape of the target. This capability becomes important when using expensive target materials (e.g. iridium for monopropellant catalysts) as we can use rectangular target foils with minimal wastage. The laser vaporization source is also far more efficient than the magnetron, consuming only milligrams/hour of target for similar beam intensities. The source can be fitted with different shape nozzles, and with nozzle extensions, to allow conditions to be optimized for different metals and cluster sizes.

The source can be run either with a



CW gas flow or with a 100 Hz pulsed valve. We have experimented with several ways of coupling the source to the beamline. One simple approach that works very well is to equip the source with a long nozzle extension, and to insert the extension directly into the end of the tapered quadrupole trap. We have had the 100 Hz source on the beamline off and on for several months now, alternating source optimization with continuing experiments using the magnetron sputter source, described below. We have made clusters from about 15 different metals now, with usable intensity (nA range). So far we have only looked at clusters in the < 15 atom range, but the trends in the mass spectra suggest that the size distributions extend to at least twice that size with reasonable intensity for most metals. (We have focused on small sizes, partly because we want to start there, and partly because the beamline can cover wide mass ranges, but only in a piece-wise fashion at present. There is no inherent problem with making the beamline scan over a wide range, however, there is no reason for a beam mass selector to have this capability, so we haven't bothered to build the computer interface that would be required).

3. Trajectory Program and Studies

To aid interpretation of the experiments, we developed a program for classical trajectory simulations of cluster impacts. The critical part of this theoretical component is the potentials used to describe the interactions. As our modeled system contains hundreds of metal atoms, it is not feasible to calculate ab initio potentials "on the fly" or to calculate an ab initio potential surface. We have adopted the approach of using empirically adjusted embedded atom potentials. The interaction potential for a given atom in the solid is calculated as the sum of a series of pair-wise potentials and an embedding term, accounting for the multi-body nature of the interaction. For the Cu-Mo system, we have adapted Cu-Cu and Mo-Mo embedding potentials from Milstein and co-workers², and have carried out an extensive series of calculations. Recently we have become concerned about a possible problem with the scaling behavior of the Milstein potential, and not having gotten any response from Milstein, we have begun to develop our own potential. This process involves doing ab initio (DFT) calculations on metal atoms and small clusters, then fitting orbital coefficients to generate the embedding parameters. Since I am not experienced in this area, we are having to feel our way along. Fortunately, for the qualitative dynamics at high impact energies, the details of the potential are probably not terribly important.

For Cu - Ni the problem with existing embedding functions is more serious, and we are having to generate a new ab initio-based potential. To provide some preliminary insight into the Cu-Ni scattering problem, we have carried out some simulations using the Cu-Mo potential with target atom masses set to that of Ni. Obviously this "pseudo-nickel" system will not correctly reproduce any effects that are potential-dependent, but it does show the (considerable) effects of the difference in masses in Cu-Mo v.s. Cu-Ni.

4. Initial Studies

Data Acquisition

To date we have worked on three systems: Cu_n^+ on molybdenum, Cu_n^+ on Nickel, and Al_n^+ on Mo. The first two are amenable to study by ESCA, and have received most of the attention. Al_n on Mo is an interesting system as we see evidence for energy and cluster size-dependent production of alumindes. Aluminide production is better studied by UPS, and we have shelved the aluminum studies until we can add a UV source to the instrument.

Our initial study was of copper deposition and implantation on molybdenum. Cu/Mo is interesting because copper and molybdenum have a large positive heat of mixing, with copper having the lower surface free energy. This means that the two metals are not normally miscible, and that deposited

²F. Milstein and S. Chantasiriwan, *Phys. Rev. B* **58**, 6006 (1998). S. Chantasiriwan and F. Milstein, *Phys. Rev. B* **53**, 14080 (1996).

copper should tend to diffuse to the surface. Only one other system (Ag^+ on Ni) with these characteristics has been studied by low energy ion beam deposition, and in that case it is found that silver migrates entirely to the surface on the experimental time scale, even at high energies where subplantation is occurring.³

The Mo target is cleaned by sputtering and e-beam annealing in the preparation chamber, and surface cleanliness is checked by XPS. Cu^+ and Cu_2^+ were prepared in the magnetron source, cooled and compressed, mass selected, then deposited on the Mo target in a 800 μm spot. Deposition coverage is varied over the range from about 0.2 to 1 monolayer (ML) equivalent, with most depositions being of about 0.5 ML, as monitored by direct measurement of the deposition ion current. Depositions were made over the impact energy range from 1 to 230 eV. 1 eV is approximately our lower limit, but we can go to considerably higher energies, if desired. The sample is then transferred to the XPS station, and the deposition spot is analyzed in small area (400 μm) mode. We also look at the ESCA spectrum at 45° to provide additional depth information. For most experiments, Mg $K\alpha$ radiation was used as this provides a large kinetic energy separation between the Cu 2p photoelectron and Cu LVV Auger peaks. In addition to these two Cu spectral regions, the Mo 3d and O 1s spectra were also acquired. A Shirley background⁴ was removed from the Mo 3d peak before integration. The Cu 2p intensities were obtained by subtracting the spectrum acquired before deposition from that acquired afterwards and fitting a Shirley background to the difference spectrum. The areas of the two spin-orbit components of the Cu peak were then obtained by integration. The Cu LVV Auger intensities were obtained by direct integration of the difference spectra. Oxygen intensity is monitored just as a check on sample cleanliness.

Three ratios of electron peak intensities provide insight into the deposition dynamics. The ratio of XPS peaks for Cu and Mo ($\text{Cu}(2p)/\text{Mo}(3d)$) provides a measure of the apparent copper concentration in the sample. This ratio is sensitive both to the amount of copper present, and to the depth distribution, as deeply buried Cu is detected with reduced efficiency because the signal is attenuated by scattering. We also measure the ratio of the Cu x-ray-induced Auger peak to the Cu photoelectron peak ($\text{CuLVV}/\text{Cu}(2p)$). This ratio is insensitive to copper concentration, but is highly sensitive to the depth distribution. This sensitivity results from the fact that the LVV electrons have ~ 3 times higher kinetic energy compared to the Cu(2p) electrons, and their mean free path, or escape depth, is roughly two times higher ($\lambda_{2p} = 7.2\text{\AA}$, $\lambda_{\text{LVV}} = 15.1\text{\AA}$). Finally, the 45° Auger/photoelectron peak ratio is, again, sensitive to the depth distribution, but scales differently with depth compared to the 0° Auger/photoelectron ratio. For copper on the surface, the Auger/XPS ratio is nearly angle-independent, but buried copper gives an angle-dependent ratio.

Data Fitting

The conventional way of fitting data such as ours is to simply fit the energy dependence of the three experimental peak ratios to some assumed function form. This approach requires assuming something about the mechanism (i.e. the functional form of the energy dependence), and furthermore, generates fitting parameters that are not related in any simple way to the physical parameters we would like to extract (sticking coefficient and depth distribution). Extracting physical insight, in essence, requires fitting the fits to a physical model.

We have taken a different approach to allow physically meaningful results to be extracted directly from the raw data. We start with a detailed simulation of the photo and Auger electron emission

³S. S. Todorov, H. Bu, K. J. Boyd, J. W. Rabalais, C. M. Gilmore, and J. A. Sprague, *Surf. Sci.* (submitted) (1998).

⁴D. A. Shirley, *Phys. Rev. B* **5**, 4709 (1972).

and attenuation in the solid. The parameters required for the simulation (emission and attenuation cross sections) are available from the literature^{51,2} or can be determined by measurements on pure Cu, Ni, and Mo samples. In the fitting, we assume one of six different types of model depth distributions (atop layer, atop clusters, buried layer, buried step, exponential decay, and truncated exponential decay). Within these models, the depth profile of copper is described by two or three parameters (sticking coefficient, characteristic depth, and profile width).

For a given model and set of parameters, we can calculate the three experimental peak ratios, and thus, fit the experiment to physically meaningful parameters describing the sticking and depth profile. Some models are not able to fit the data at all, and therefore we can rule out the corresponding deposition mechanisms. In some cases, more than one model yields reasonable fits, and this simply tells us the limits of our experimental sensitivity to details of the depth distributions.

The difficulty in this fitting process is that the relation between the fitting parameters and the calculated peak ratios is not analytic, thus the usual least-squares fitting procedure cannot be applied. We have developed a program using a metropolis-based simulated annealing algorithm to locate the best fit, using the cumulative RMS error as the prescription for searching parameter space. We first attempted a direct fit, allowing the sticking, depth, and width parameters to vary independently at each experimental energy, subject to penalty factors to force a smooth fit. This is roughly equivalent computationally, to trying to find the global minimum on a 50 to 75 dimensional surface, and proved infeasible. The fits shown below assume a simple bi-linear energy dependence for the parameters, thus reducing the parameter space substantially.

Experimental Results and Fits

The experimental peak ratios for deposition of Cu^+ and Cu_2^+ on Mo are shown in Figure 4, along with fits and the extracted fit parameters. It should be noted that these are very small signal experiments, as we are looking at weak transitions (e.g. x-ray-induced Auger) for sub-monolayer doses of light metals, much of which is buried or backscattered. In the figure, Mo/CuCalc and Mo/CuEXP refer to the simulated and experimental Mo(3d)/Cu(2p) photoelectron peak ratio, A/X refers to the copper Auger/photoelectron peak ratio calculated and experimental, at 0° and 45° takeoff angles. It is possible to get reasonable fits to the data with several model depth distributions, and the results for the truncated exponential are shown. This model has the maximum Cu concentration in the surface layer, with an exponential decay into the bulk, truncated at a variable depth. Good fits are also achieved for a buried step model, where there is a Cu-containing layer of variable thickness, starting at a variable depth. Note however, that in the truncated exponential, the decay depth parameter is large enough compared to the truncation depth, that the shape of the profile is approximately that of a step starting at the surface with width equal to the truncation depth. Furthermore, the start depth in the buried step model is nearly zero, thus, the two models are actually describing quite similar depth distributions. Just as important, the fitting clearly rules out the atop distributions (atop layer and atop clusters) as these models are not able to reproduce the change in Auger/XPS ratios with energy and angle.

Broadly speaking, the conclusions of the fitting are:

Cu^+ deposition:

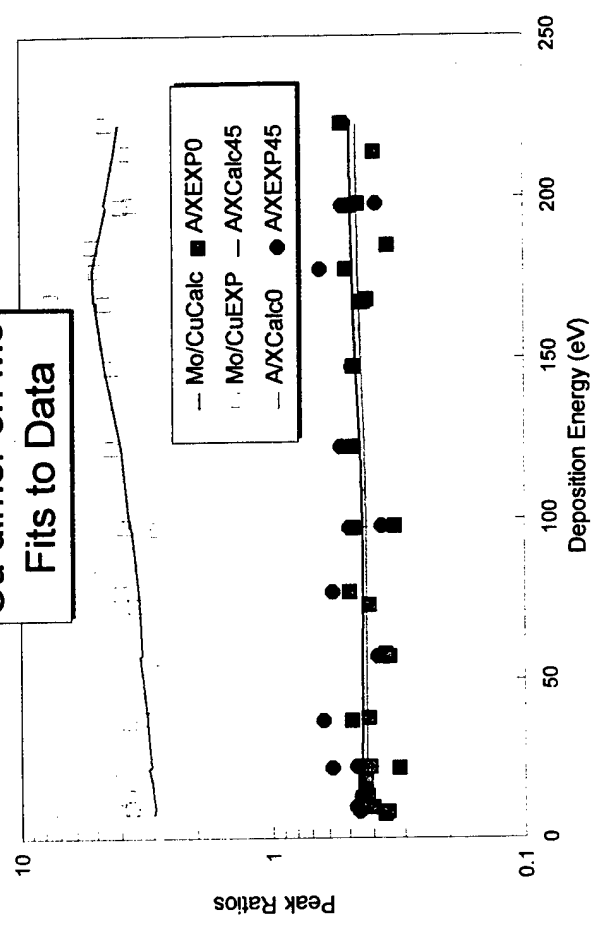
Sticking coefficient declines from ~100% at low energies to ~50% at ~100 eV

Cu_2^+ deposition

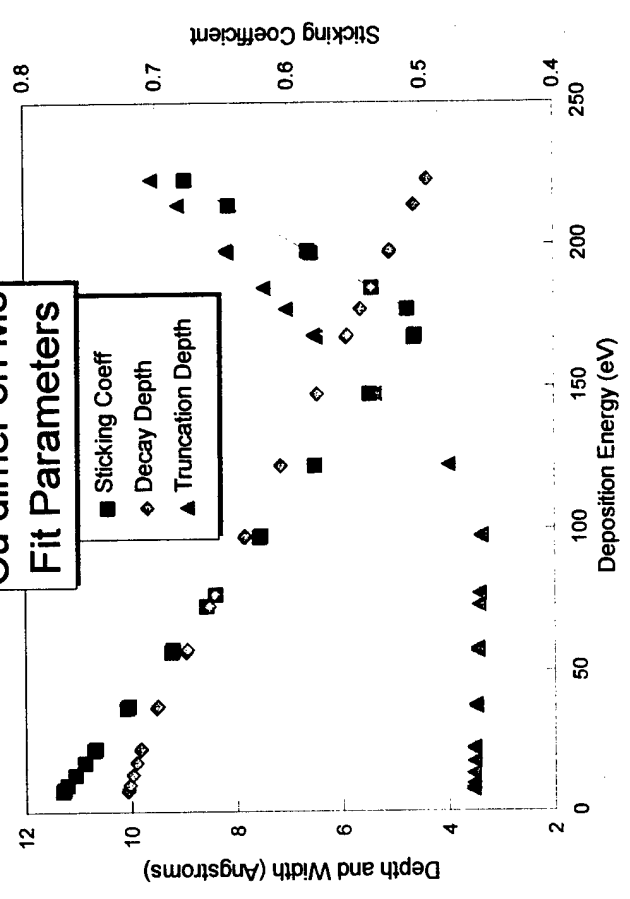
Sticking coefficient declines from ~75% at low energies to ~50% at ~100 eV

⁵S. Tanuma, C. J. Powell, and D. R. Penn, *Surf. Interf. Anal.* **17**, 911 (1991); J. F. Moulder, W. F. Stickle, P. E. Sobol, K. D. Bomben, and J. J. Chastain & R. C. King, eds., *Handbook of X-ray Photoelectron Spectroscopy* (Physical Electronics, Eden Prairie, MN, 1995).

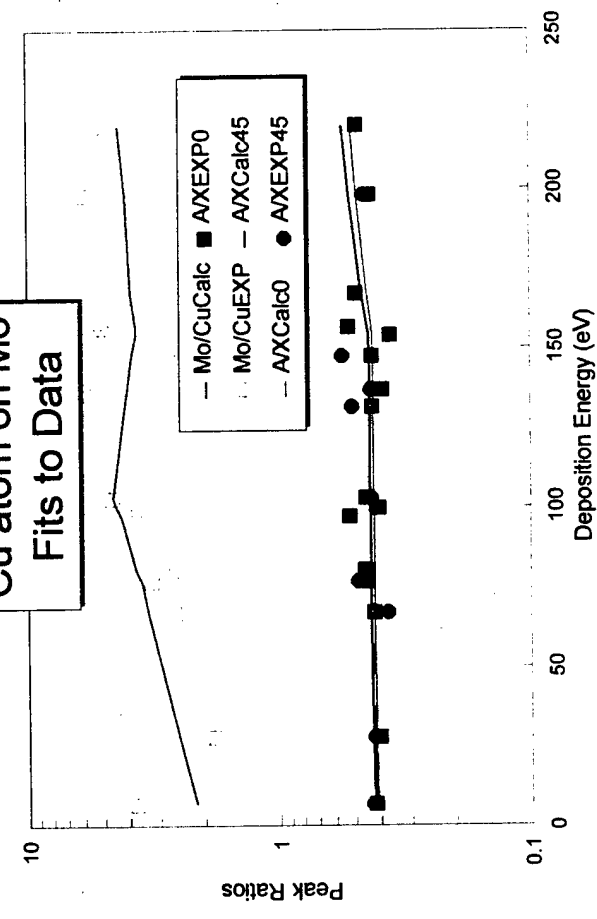
Cu dimer on Mo
Fits to Data



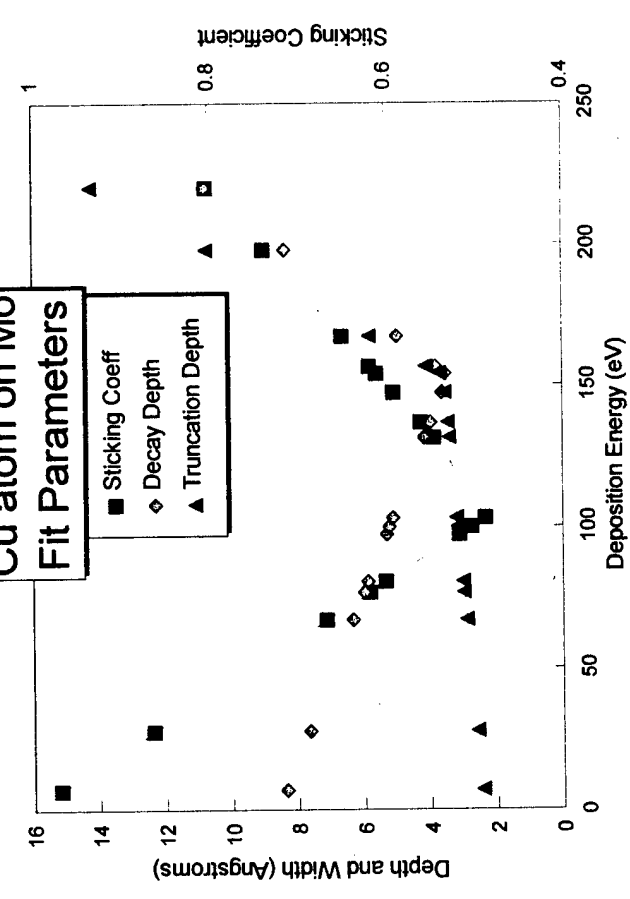
Cu dimer on Mo
Fit Parameters



Cu atom on Mo
Fits to Data



Cu atom on Mo
Fit Parameters



All copper is at surface up to ~ 150 eV. (truncation depth \approx atomic diameter)

At higher energies, stable subplanted copper is found (truncation depth increasing)

Even at high energies, copper intensity peaks in the surface region

Rise in sticking coefficient at high energies is roughly coincident with onset of subplantation

All copper is at surface up to ~ 100 eV. (truncation depth \approx atomic diameter)

At higher energies, stable subplanted copper is found (truncation depth increasing)

Even at high energies, copper intensity peaks in the surface region

Rise in sticking coefficient at high energies is roughly coincident with onset of subplantation

The principle differences between atomic and dimer impacts are reduced low energy sticking for the dimer, and a lower threshold for subplanted copper for the dimer.

Figures 5 and 6 summarize the trajectory simulation results. These distributions are based on roughly 150 trajectories at each energy, requiring about three weeks of computer time. For Cu^+ , the simulations show no evidence of penetration at 25 or 50 eV, and very slight penetration at 100 eV. This suggests that the absence of subplanted copper at 100 eV (roughly twice the Mo displacement threshold energy) is not the result of back-diffusion to the surface, but simply reflects no penetration. In good agreement with experiment, the simulations show the onset of penetration at 150 eV, with most material remaining in the near-surface layer. At 200 eV, there is substantial penetration, in agreement with experiment. In fact, about half the trajectories lead to penetration clear through the seven layer slab of Mo (110) that serves as the target in the simulation. Perhaps the biggest disagreement between experiment and simulation is the lack of significant backscattering (i.e., high sticking probability) for all energies. This probably reflects the fact that we stop the trajectories after only a picosecond or two, and at that point the target slab is still hot enough that evaporation of surface atoms is not unlikely. It is simply not feasible to run the trajectories long enough to observe post-impact thermal processes like desorption or diffusion.

The simulations for Cu_2^+ impact are somewhat different. Most copper is found in the near-surface region over most of the energy range, but in a broader distribution, that includes some penetration even at low energies. This is not inconsistent with experiment, when the possibility for Cu desorption is included. Desorption would tend to deplete the surface copper, leaving a distribution more heavily weighted towards penetration. Note that deep penetration is first observed for Cu_2^+ at 100 eV. The simulations, thus, are consistent with the experimental finding that deep penetration sets in at ~ 100 eV for dimers, compared to ~ 150 eV for Cu^+ . Because the depth distributions are likely modified by post-impact thermal processes, and because our model depth profiles for the experimental fitting are very simple functions, it is not possible to directly compare simulation and fit parameters. We are in the process of checking to see if the simulated profiles can fit the experimental data directly.

An interesting question for dimer deposition is the correlation of the two atoms' final positions. It turns out that the, by far, most common arrangement is for one atom to penetrate into the first or second target layer, with the second atom remaining on the surface nearly on top of the subplanted atom.

One important conclusion is that subplanted copper is stable in Mo, despite the thermodynamic driving force for diffusion of Cu to the surface. We have attempted to anneal the samples, trying to measure the activation energy for diffusion. Unfortunately, the desorption temperature of Cu from Mo is only about 700 K, and at lower temperatures the diffusion is immeasurably slow.

Cu^+ and Cu_2^+ on Nickel

We have almost completed a full set of data for Cu^+ and Cu_2^+ on Ni(100) and polycrystalline nickel. This system is similar to Cu/Mo in that copper migration to the surface is thermodynamically favored, although the free energy of mixing is substantially smaller, as is the difference in surface

Trajectory Summary

Depth distribution Cu^+ - Mo

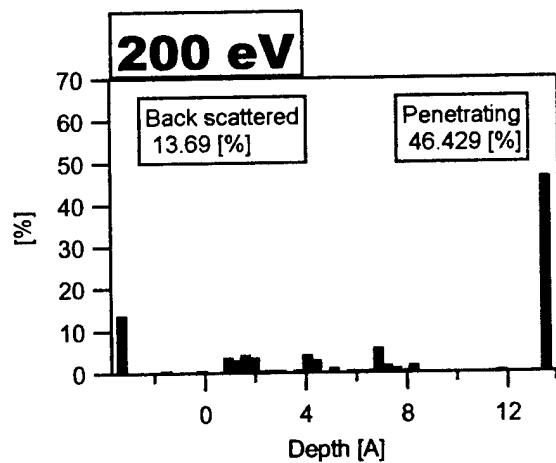
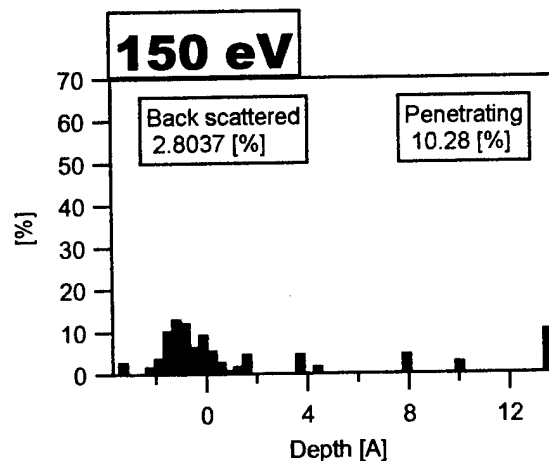
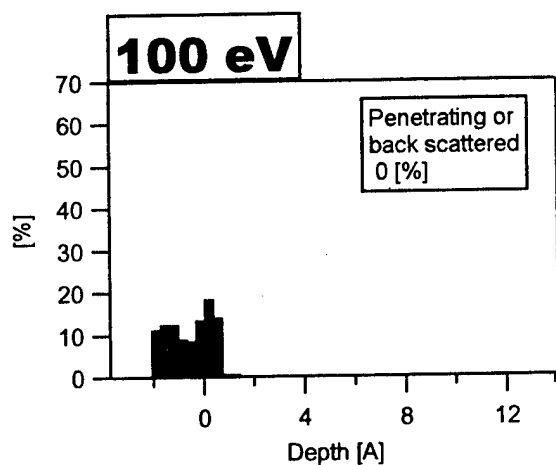
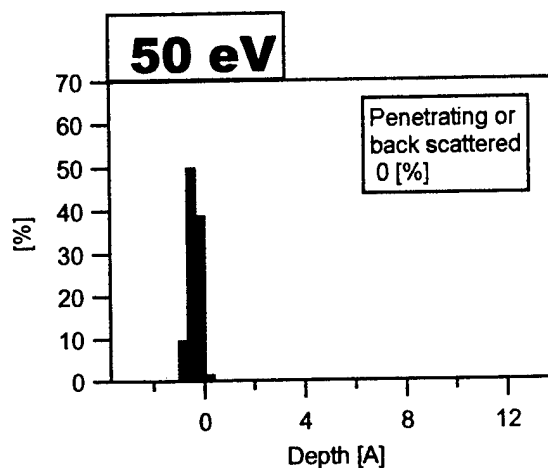
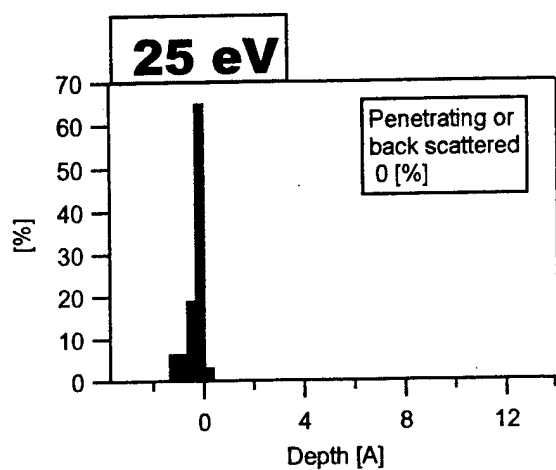
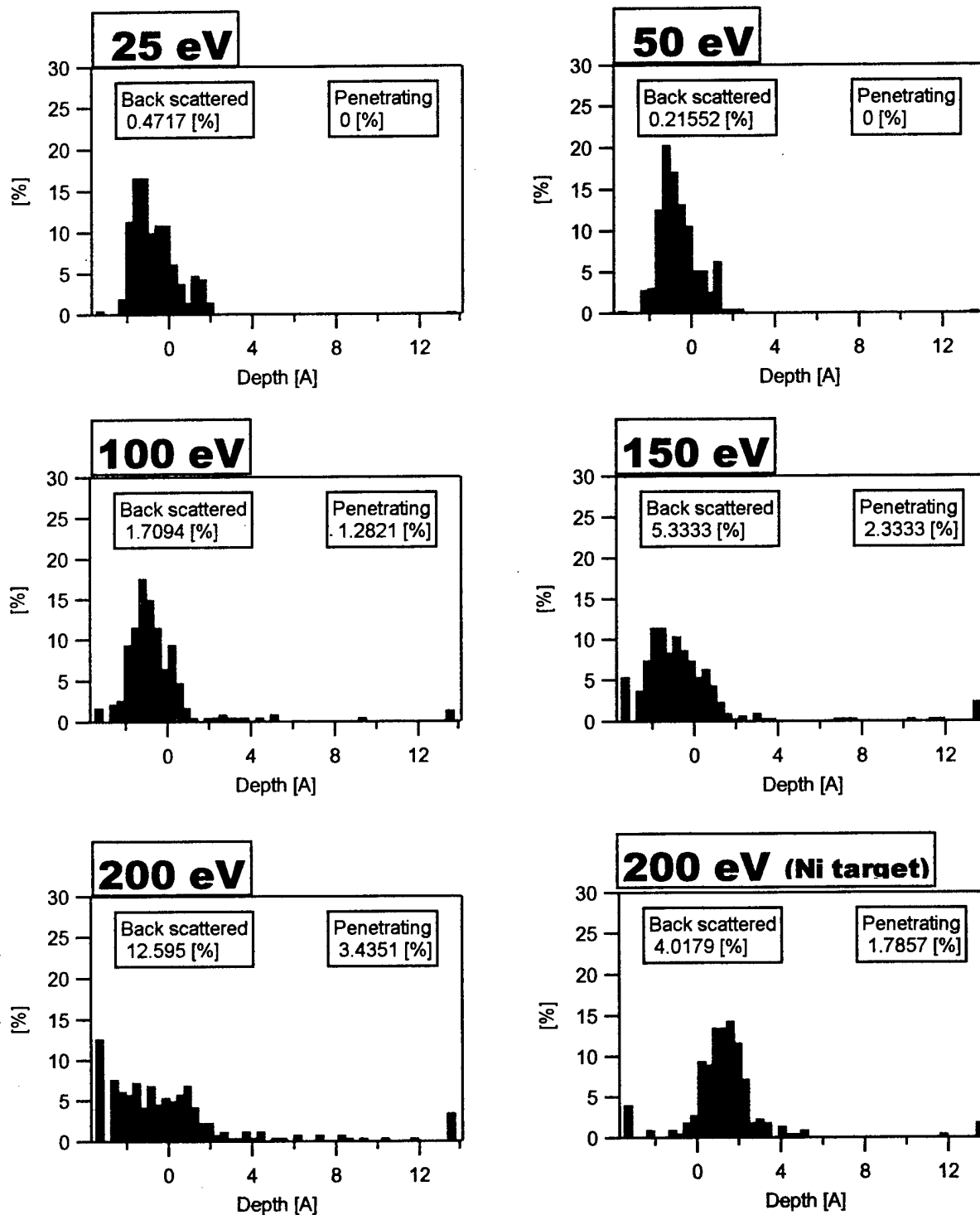


Fig 5

Trajectory Summary

Depth distribution Cu_2^+ - Mo



energies. As of this date, I have fit only the Cu_2^+ on Ni(100). The results are strikingly different from Cu_2^+ on Mo in several ways. The most obvious difference is that the apparent sticking coefficients are much lower on nickel – roughly 25%, independent of energy. I use the term “apparent sticking coefficient” because the low Cu signal could indicate either that copper is backscattering or desorbing from the nickel surface, or possibly that some copper is penetrating so deeply into the nickel that no signal is observed. The latter possibility is rather unlikely in light of the thermodynamics, particularly at low energies, but we are planning to check for deep copper using TOF-SIMS, available in our department. This technique is extremely sensitive and can resolve depth distributions on a roughly 10 Å scale. It is interesting to note that for polycrystalline Ni (should be mostly 111 surface) the apparent sticking coefficient is closer to 50%.

The other major difference is that the best fits for Cu_2^+ in Ni(100) are with the atop layer model, which failed miserably for Cu and Cu_2 on Mo. This suggests that what little copper is present in the observable depth range of the nickel surface is found on top of the nickel surface. Atop is not surprising at low impact energies, but we expect substantial penetration at high energies. The implication seems to be that shallowly subplanted copper is able to diffuse back to the surface for nickel, but not for molybdenum.

Because of the lack of a good Cu-Ni embedding potential (see above) we have only simulated copper on “pseudo-nickel”, i.e., a target with nickel mass, but molybdenum structure and potential. The result for 200 eV is shown in figure 6 at the lower right corner. Note that in comparison with the Mo target at 200 eV (lower left) there is substantially less copper left on the surface, substantially more in the first few subsurface layers, and virtually no deep penetration. This result is consistent with the experiment, in the sense that copper subplanted into the first few target layers is most likely to be able to diffuse to the surface, producing atop copper, as is observed.

Summary

A unique cluster ion deposition/surface chemistry instrument has been constructed and its operation has been demonstrated with several test systems. Two different cluster ion sources have been constructed and demonstrated. An embedded atom trajectory simulation program has been written and used in theoretical studies that complement the experiments. At present only two publications have resulted from the work described (see below), however, I anticipate about three more publications based on existing results. One each will cover Cu_n^+ on Mo and on Ni, and one will discuss our embedding program and new potentials.

Publications in print:

“A phase-space-compressing, mass-selecting beamline for focused ion beam production”, Kevin J. Boyd, Adam Łapicki, Masato Aizawa, and Scott L. Anderson, *Rev. Sci. Instrum.*, 69 (1998) 4106-15.

“Cluster-surface collisions by phase-space compressed guided ion beam methods”, Kevin J. Boyd, Adam Łapicki, Masato Aizawa, and Scott L. Anderson, *Nuc. Inst. Meth. Phys. Res. B* 157 (1999) 144-54

Presentations at meetings:

Invited:

“New tricks for cluster ions beam deposition”, Gordon Conference on Atomic and Molecular Clusters, Ventura, CA, Jan 4-9, 1998

“Cluster-Surface Collisions by Phase-Space Compressed Guided-Ion Beam Methods”, The Twelfth International Workshop on Inelastic Ion-Surface Collisions, South Padre Island, Jan 24-29, 1999

Contributed:

"A phase-space-compressed, guided-ion beam instrument for mass-selected ion beam deposition", Adam Łapicki, Kevin J. Boyd, Masato Aizawa, and Scott L. Anderson, 44th AVS National Symposium, San Jose, Oct. 20-24, 1997.

"Film/Substrate interfacial interactions by mass-selected cluster ion deposition", Kevin J. Boyd, Adam Łapicki, Masato Aizawa, and Scott L. Anderson, 44th AVS National Symposium, San Jose, Oct. 20-24, 1997

"A phase-space compressed, guided ion beam instrument in studies of mass-selected ion beam deposition and interfacial interactions between nanoscale clusters and substrate surfaces" Adam Lapicki, Kevin J. Boyd, Masato Aizawa, and Scott L. Anderson, International Symposium on Nano-scale Modifications of Surfaces, Krakow, May 1998.

"Dynamics of Cu^+ and Cu_2^+ impact on molybdenum", Kevin J. Boyd, Adam Łapicki, Masato Aizawa, and Scott L. Anderson, Gordon conference on the Structures, Energetics, and Dynamics of Gaseous Ions, Ventura, Feb 28-Mar 5, 1999.